

JGR Space Physics

RESEARCH ARTICLE

10.1029/2019JA027538

Key Points:

- Ionospheric ion upflow occurrence exhibits a dawn-dusk asymmetry, consistent to that of the Region 1 field-aligned currents
- The ion upflow occurrence expands to a wider area in disturbed times than in quiet times
- In both hemispheres, maximum ion upflow occurrence is consistent with cusp and nightside auroral disturbance regions

Supporting Information:

- Figure S1

Correspondence to:

Q.-H. Zhang,
zhangqinghe@sdu.edu.cn

Citation:








Ma, Y.-Z., Zhang, Q.-H., Jayachandran, P. T., Oksavik, K., Lyons, L. R., Xing, Z.-Y., et al. (2020). Statistical study of the relationship between ion upflow and field-aligned current in the topside ionosphere for both hemispheres during geomagnetic disturbed and quiet time. *Journal of Geophysical Research: Space Physics*, 125, e2019JA027538. <https://doi.org/10.1029/2019JA027538>

Received 14 OCT 2019

Accepted 11 AUG 2020

Accepted article online 25 AUG 2020

Statistical Study of the Relationship Between Ion Upflow and Field-Aligned Current in the Topside Ionosphere for Both Hemispheres During Geomagnetic Disturbed and Quiet Time

Yu-Zhang Ma¹ , Qing-He Zhang¹ , P. T. Jayachandran² , Kjellmar Oksavik^{3,4} , L. R. Lyons⁵ , Zan-Yang Xing¹ , Shan-Yu Zhou¹, Marc Hairston⁶ , and Yong Wang¹ 

¹Shandong Provincial Key Laboratory of Optical Astronomy and Solar-Terrestrial Environment, Institute of Space Sciences, Shandong University, Weihai, China, ²Physics Department, University of New Brunswick, Fredericton, New Brunswick, Canada, ³Birkeland Centre for Space Science, Department of Physics and Technology, University of Bergen, Bergen, Norway, ⁴Arctic Geophysics, University Centre in Svalbard, Longyearbyen, Norway, ⁵Department of Atmospheric and Oceanic Sciences, University of California, CA, Los Angeles, USA, ⁶William B. Hanson Center for Space Sciences, University of Texas at Dallas, Richardson, TX, USA

Abstract A statistical study of ion upflow and field-aligned currents (FACs) has been performed in the topside ionosphere of both hemispheres for magnetic quiet and disturbed times by using DMSP satellite observations from 2010–2013. Distributions in MLT/MLat reveal that ion upflow occurrence shows a dawn-dusk asymmetry distribution that matches well with the Region 1 FACs. In addition, there are highest occurrence regions near noon and within the midnight auroral disturbance area, corresponding to dayside cusp and nightside auroral disturbance regions, respectively. Both the ion upflow occurrence and FAC regions expand equatorward to a wider area during disturbed times.

1. Introduction

It is a common view that the ionosphere and magnetosphere are coupled through the plasma convection and currents. Additionally, the high-latitude ionosphere is an important source of magnetospheric plasma, and ion upflow plays a significant role in the coupled ionosphere-magnetosphere system (Chappell, 1988; Chappell et al., 2000; Horwitz & Moore, 1997; Moore et al., 1999; Shelley et al., 1972, 1976a, 1976b). Ion upflow can occur from 200 km altitude to several Earth radii (R_E) (Abe et al., 1993; Li et al., 2012, 2013; Liu et al., 2001; Nilsson et al., 2013; Ogawa et al., 2009), especially in the aurora oval and cusp region (Andersson et al., 2004; Coley et al., 2006; Heelis et al., 1992; Loranc et al., 1991; Øieroset et al., 1999), with maximum occurrence near magnetic noon and midnight (Ogawa et al., 2009, 2010). Distributions of ion velocity, ion temperature, and occurrence rate of ion upflow have also been studied (Abe et al., 1993; Endo et al., 2000). Studies reveal that there is a greater probability of observing ion upflow events on the nightside than on the dayside (Zhao et al., 2017), and the occurrence rate is highest for high geomagnetic activity (Coley & Heelis, 2009; Zhao et al., 2014, 2016). There is also a dawn-to-dusk asymmetry, with a higher occurrence of ion upflow on the dawn side than on the dusk side during quiet times and a higher occurrence on the dusk side than on the dawn side during storm time (Liang, 2006; Liu et al., 2001).

Different generation mechanisms of ion upflow have been investigated through observations and simulations (Horwitz & Moore, 1997; Liu et al., 2001; Qing-He et al., 2016; Zhang et al., 2017). These mechanisms include (1) Joule dissipation; (2) increased upward ambipolar electric field with soft electron precipitation; (3) heating due to convection shear; (4) ring current ion precipitation (Ganguli et al., 1994; Heelis et al., 1993; Liu & Lu, 2004; Strangeway et al., 2005; Whitteker, 1977; Yeh, 1990).

Field-aligned currents (FACs), which couple the magnetosphere and ionosphere, were first proposed in 1908 (Birkeland, 1908) and were first observed by spacecraft in 1966 (Zmuda et al., 1966). Iijima and Potemra (1976) separated the high-latitude current system into Region 1 FACs, which flow into the ionosphere on the dawn side and out of the ionosphere on the dusk side, and Region 2 FACs, which are located further equatorward and flow reversely to Region 1. There is also some evidence that the FAC distribution may have a morning-afternoon asymmetry based on EISCAT incoherent-scatter radar observations

(Fontaine & Peymirat, 1996). Shi et al. (2010) also found some asymmetries between the Northern and Southern Hemispheres.

The FACs are important for the transport of energy and momentum from the solar wind to the magnetosphere/ionosphere. They are also important for Joule and particle heating, which are known to generate ion upflow (Akasofu & Kan, 2013; Fujii et al., 1990; Gurnett & Frank, 1973; Potemra, 2013; Torbert et al., 1981). However, to our knowledge, no study has yet documented a statistical relationship between FACs and ion upflow. Despite many statistical and event studies on either ion upflow or FACs (Shen et al., 2016), there is still a knowledge gap regarding the occurrence of ion upflow in relation to FACs during magnetic quiet and disturbed times. Nevertheless, the relationship between FACs and ion upflow is essential for a deeper understanding of magnetosphere-ionosphere coupling. In this paper, we therefore utilize DMSP satellite data during magnetic disturbed and quiet times to study the statistical and morphological characteristics of, and relationships between, ion upflow occurrence and FACs in both hemispheres during a 4-year period (2010 to 2013).

2. Data and Method

2.1. Data Processing

The DMSP satellites operate in sun-synchronous polar orbits at about 850 km altitude, with 98.7° inclination and orbital period of approximately 101 min. The data used in this study come from DMSP F16 and include the following data sets: (1) special sensor for ions, electrons, and scintillation (SSIIES) that provide density, temperature, and velocity data at 4 s time resolution for the thermal plasma in the topside ionosphere; (2) Special Sensor for Precipitating Particles (SSJ-4) that provide fluxes and energy spectra of precipitating electrons and ions at 1 s time resolution in the energy range of 30 eV to 30 keV in logarithmically spaced energy steps (Hardy et al., 1984); (3) spatial magnetic field detectors (SSM) that consist of triaxial fluxgate magnetometers that measure the magnetic field fluctuations in a range of $\pm 65,535$ nT and resolution of 1 s and 2 nT (Rich & Hairston, 1994).

The FAC is derived by performing a minimum variance analysis (MVA) to determine the field-aligned coordinates of the SSM data, where \mathbf{l} , \mathbf{m} , and \mathbf{n} are along the maximum, intermediate, and minimum variance directions, respectively (Khrabrov & Sonnerup, 1998a, 1998b; Sonnerup & Jr, 1967). We also assumed that the FAC is a stable current sheet during the satellite crossing (Luhr et al., 1996). After conversion to field-aligned coordinates, the FAC can be calculated by subtracting the IGRF model magnetic field and using Ampere's law to solve the curl-B equation. For single-point measurements like DMSP, Luhr et al. (1996) and Wang et al. (2005) suggested converting the observations into spatial gradients by considering the velocity and assuming stationary of the current during the satellite passage. The dB_m is zero under the SSM coordinates and a thin current sheet assumption. The FAC can then be derived as the following:

$$\mu_0 j_{//} = (\nabla \times B)_{//} = \frac{dB_l}{dm} - \frac{dB_m}{dl} = \frac{DB_l}{v_{sc,m}} - \frac{DB_m}{v_{sc,l}} = \frac{DB_l}{v_{sc,m}} \quad (1)$$

where

μ_0 : permeability in a vacuum;

$j_{//}$: FAC;

dB_m, dB_l : the m and l components of the magnetic field;

DB_m, DB_l : the magnetic disturbance derived from SSM data, equal to dB_m, dB_l ;

$v_{sc,m}$: m component of the satellite velocity in field-aligned coordinates derived from SSIIES data using the MVA method; and

$v_{sc,l}$: l component of the satellite velocity in field-aligned coordinates derived from SSIIES data using the MVA method.

2.2. Identification of Upflow Events

The ion velocity or flux can be used as a criterion to identify ion upflow events (Keating et al., 1990). The satellite can observe the ion velocity in the vertical (positive directed upward) and cross-track (positive

directed toward the left of the satellite motion) directions. In this paper, the measured ion velocities were projected in the directions parallel and perpendicular to the magnetic field based on DMSP SSM measurements. At about 850 km altitude, the field-aligned ion velocity V_{\parallel} (upward is positive) is usually lower than 200 m/s, unless there is extra acceleration (Endo et al., 2000). We therefore use 200 m/s as a lower threshold for identification of ion upflow as selected by Keating et al. (1990) before.

2.3. The Temporal and Spatial Data Coverage

This statistical study uses DMSP F16 data during magnetic quiet and disturbed times in 2010–2013. Magnetic quiet and disturbed times are derived based on the 10 most quiet and five most disturbed days of each month in the Helmholtz-Zentrum Potsdam Kp data set. Figure 1 shows the monthly averaged Kp index (summed over 24 hr intervals) for the quiet and disturbed days. The dots are the average of the values, and the shadows indicate their standard deviation. Up to 480 quiet and 240 disturbed days are considered, and all DMSP F16 orbits have been surveyed to identify the upflow events.

Based on the ion velocity criteria in section 2.2 and using only data of quality 1 (best quality: the O^+ fraction is more than 85% and the total ion density is more than $1,000 \text{ cm}^{-3}$), we identified a total of 1,064,820 upflow event data points. In the Northern Hemisphere, there were 329,485 and 273,219 data points for quiet and disturbed times, respectively. In the Southern Hemisphere, there were 234,268 and 227,848 data points for quiet and disturbed times, respectively.

We calculated the FACs for all data points together with the corresponding magnetic latitude (MLat) and local time (MLT), which were obtained from the SSJ/4 data. Next, we binned all data in grid cells of $1^\circ \text{ MLat} \times 0.5 \text{ hr MLT}$ for $60\text{--}90^\circ \text{ MLat}$, depending on hemisphere and geomagnetic activity level. To avoid fringe effects due to insufficient data coverage, we excluded grid cells that had less than 400 data points.

3. Results

Figure 2 shows the statistical occurrence of ion upflow events and FACs in both hemispheres for geomagnetic quiet times. The left column displays the data in the Northern Hemisphere, and the right column displays the data in the Southern Hemisphere. The panels show the data coverage, the upflow occurrence, the FAC, and regression analyses of the upflow occurrence versus the intensity of Region 1 FACs. The pink contours of the upflow occurrence from Figures 2c and 2d have been overlaid in Figures 2e and 2f to facilitate comparison. The data coverage in Figures 2a and 2b maximizes in the Northern Hemisphere dayside and the Southern Hemisphere nightside due to the DMSP F16 orbit. However, over time, a wide area of both hemispheres is well covered. In Figures 2g and 2h, the x axis is reversed to correspond with the FACs distribution. The blue data points refer to the downward Region 1 FACs, and the red ones refer to the upward Region 1 current. The Region 1 current is identified as the upward/downward current on the dusk/dawn side and should be poleward of the Region 2 current, which is downward/upward current pair in dusk/dawn side. Lines give linear fits, and the parameters of each fit are given above each part, where R is the Pearson's correlation between upflow rate and magnitude of FACs. The pink dash lines show with double standard derivation ($\text{fits} \pm 2\Delta$) errors of the fitted curves.

The upflow occurrence in Figure 2c shows a clear dawn-dusk asymmetry in the Northern Hemisphere with a higher occurrence rate in the morning sector. The highest occurrence rate ($>30\%$) appears around noon (about $10\text{--}14 \text{ MLT}$ and 80° MLat), which may be associated with the cusp/cleft fountain (Lockwood et al., 1985). Because of the gap in the satellite coverage of the cusp region of the Southern Hemisphere, it is not possible to state definitely whether the upflow occurrence there is symmetric or asymmetric. But the increased upflow occurrence at 80° MLat and 9 MLT suggests an asymmetric distribution toward the dawnside that is similar to what is observed in the Northern Hemisphere. Also, it shows the highest occurrence rate in two regions: the area around 80° MLat and 9 MLT mentioned before that is associated with the cusp/cleft fountain and around midnight (72° MLat and 0 MLT) that is most likely associated with nightside particle precipitation.

In Figures 2e and 2f, blue denotes downward FACs, and red represents upward FACs. The distribution of these currents is consistent with Region 1 and Region 2 FACs (Iijima & Potemra, 1978). Note that the area of high ion upflow occurrence (highlighted by pink contours) appears to coincide very well with the area of Region 1 FACs where the currents are mainly downward in the dawnside sectors and upward in the

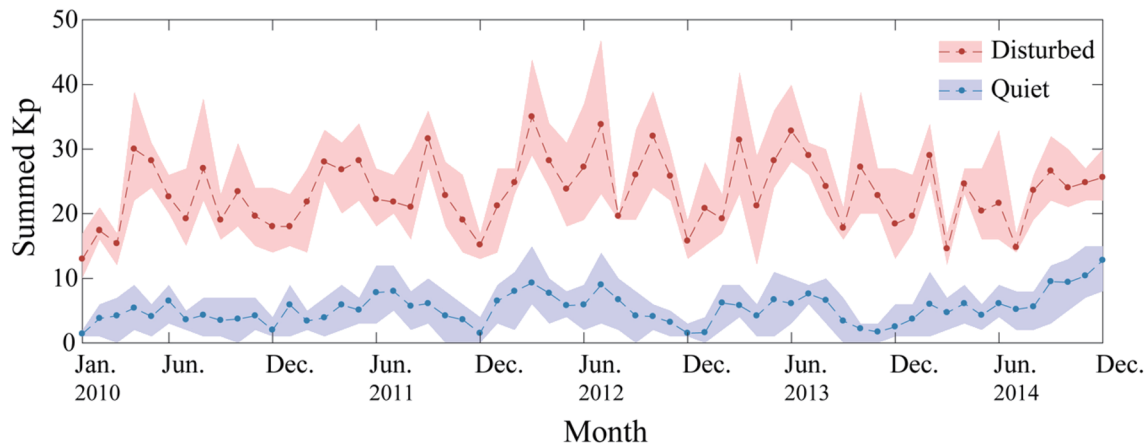


Figure 1. Monthly averaged Kp index (summed over 24 hr intervals) for the quiet and disturbed days that is used for event selection. The shading indicates the error bars.

duskside sectors. This suggests that Region 1 FACs are an important area for ion upflow during geomagnetic quiet times, and the electron heating associated with soft electron precipitation (not shown) may contribute to the ion upflow. Figures 2g and 2h show a relatively significant linearity between the upflow occurrence and Region 1 FACs, especially on the dawnside where the correlation is much higher than that on the dusk side. This may be due to more heating sources on the dawnside: the higher convection speed (ion frictional heating) and soft electrons precipitation (electron heating, not shown) observed in the dawn sections.

Figure 3 is in the same format as Figure 2 but for geomagnetic disturbed times. The ion upflow occurrence and FACs have many similar features with the quiet times. The polar edge displays a similar behavior, but the low-latitude boundary expands nearly 10° equatorward during disturbed times. Moreover, the dayside dawn-to-dusk asymmetry in ion upflow occurrence (Figures 3c and 3d) becomes more obvious in both hemispheres, and there is an expansion of the region on the nightside. Nevertheless, the ion upflow occurrence still matches very well with the location of Region 1 FACs, and the highest occurrence rate is located within the downward Region 1 FACs in the morning sector (Figures 3e and 3f). However, the correlation between Region 1 FACs and the upflow occurrence shows slightly weaker linearity than that during quiet times (Figures 3g and 3h). In addition, the downward current generally has a higher correlation with ion upflow occurrence than does the upward current in the Southern Hemisphere, which may be due to the combined contribution of stronger convection speed and soft electron precipitations (not shown). In the Northern Hemisphere, the situation is opposite: Upward current has higher correlation than downward current, this perhaps being caused by the stronger electron precipitation in the dusk sections (not shown).

4. Conclusion and Discussion

We have investigated the distribution of occurrence of both ion upflow and FACs as well as a statistical comparison between these two parameters during magnetic quiet and disturbed times by DMSP F-16 satellite observations from 2010–2013. A dawn-dusk asymmetry is clearly seen in the distribution of ion upflow occurrence in the Northern Hemisphere, and possibly, a similar asymmetric distribution appears in the Southern Hemisphere, which is consistent with previous results (Liang, 2006; Liu et al., 2001). In both hemispheres, the ion upflow occurrence is higher on the dawn side, where the associated convection speeds, and thus fractional heating, have been observed to be greater than that on the dusk side (Ma, Zhang, Xing, Heelis, et al., 2018; Ma, Zhang, Xing, Jayachandran, et al., 2018). The highest occurrence rates are seen in the cusp region and the nightside auroral oval. The topology of the FACs distribution is very similar to previous studies (Iijima & Potemra, 1976, 1978), but the magnitude of currents is also presented in the current study. Comparing the result between magnetic quiet and disturbed times, the higher values of both FACs and ion upflow occurrence expand to cover larger areas, with the low-latitude boundary expanding nearly 10° equatorward. There is also a more obvious dawn-dusk asymmetry during disturbed times.

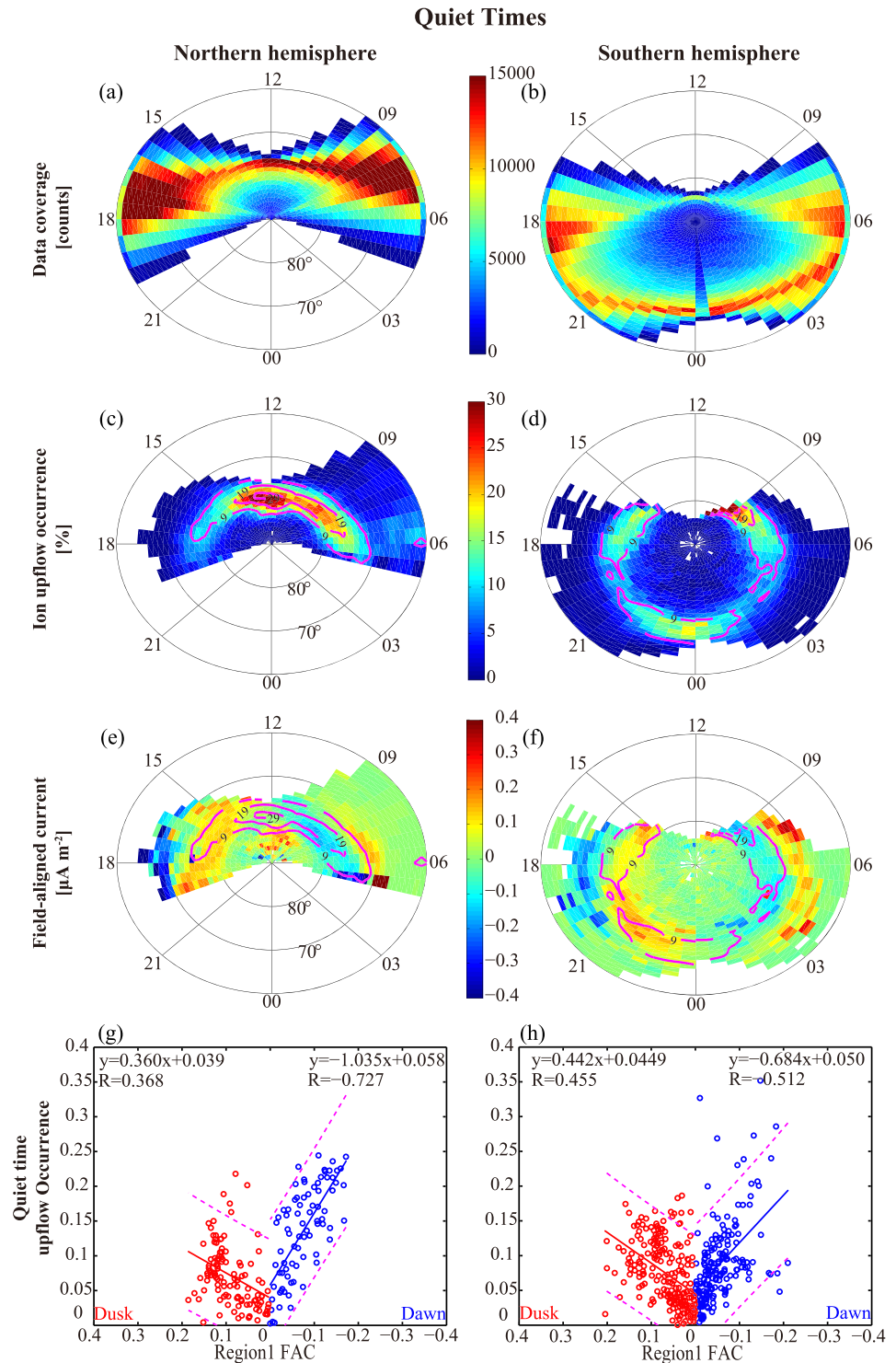


Figure 2. Statistical results in both hemispheres for magnetic quiet times. Panels from top to bottom show (a and b) data coverage, (c and d) ion upflow occurrence, (e and f) FACs, and (g and h) the regression analysis of the ion upflow and FACs for showing the relation between the upflow occurrence and Region 1 FACs in each hemisphere.

Unexpectedly, the distribution of high ion upflow occurrence was found to be consistent with the area of Region 1 FACs in both hemispheres. The areas of ion upflow coincide well with the area of the downward Region 1 FACs on the dawnside and upward Region 1 FACs on the duskside. However, the correlation is

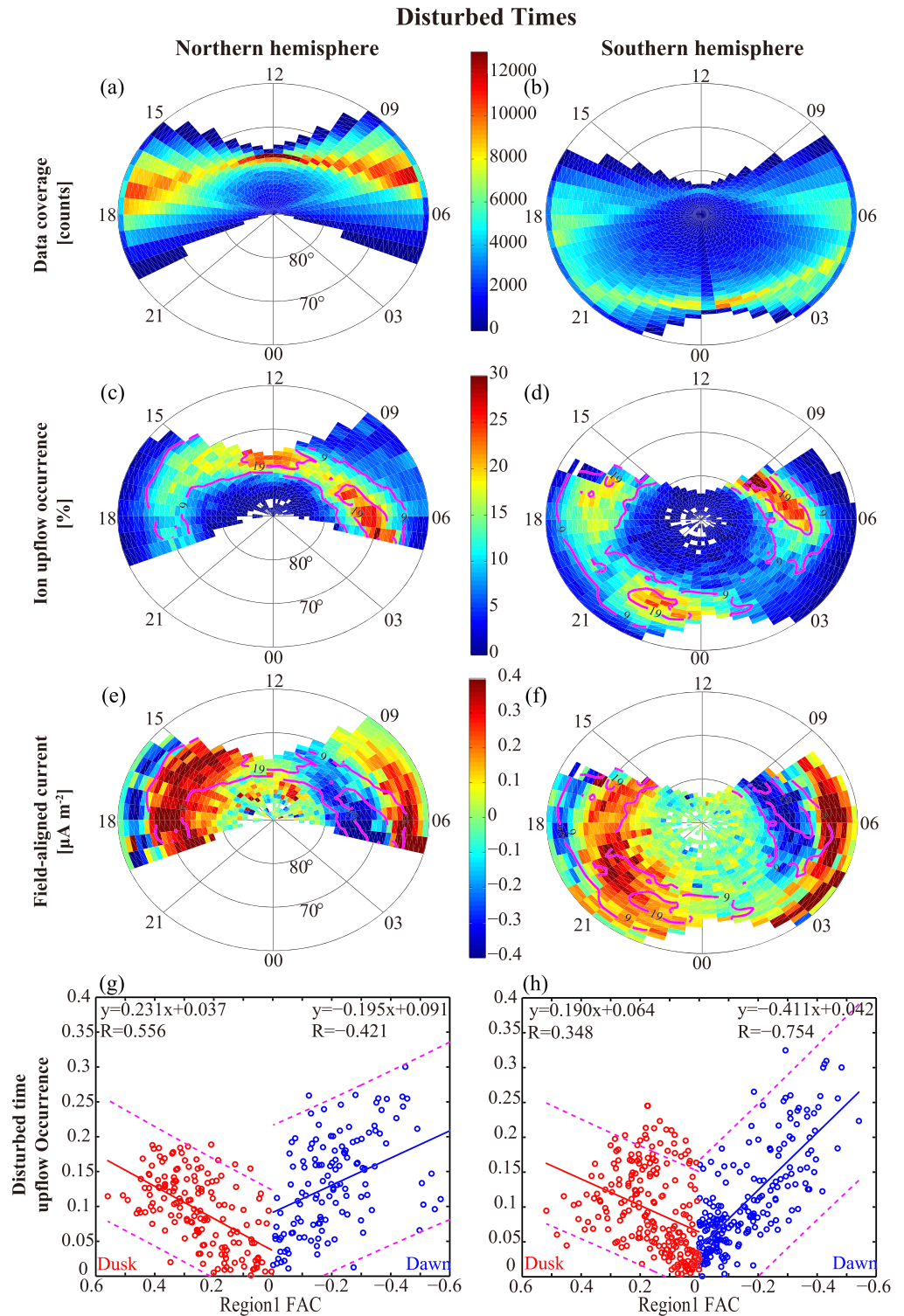


Figure 3. Same format as Figure 2 but for magnetic disturbed times.

much higher on the dawnside than on the duskside. It is important to learn what leads to this coincidence. On the dawnside, the basic physical connection between ion upflow and downward FACs might be related to Poynting flux (not shown, due to lack of accuracy observations of electric field or velocity to calculate them) and ion heating, which are believed to lead to ion upflow due to the ion-neutral frictional heating

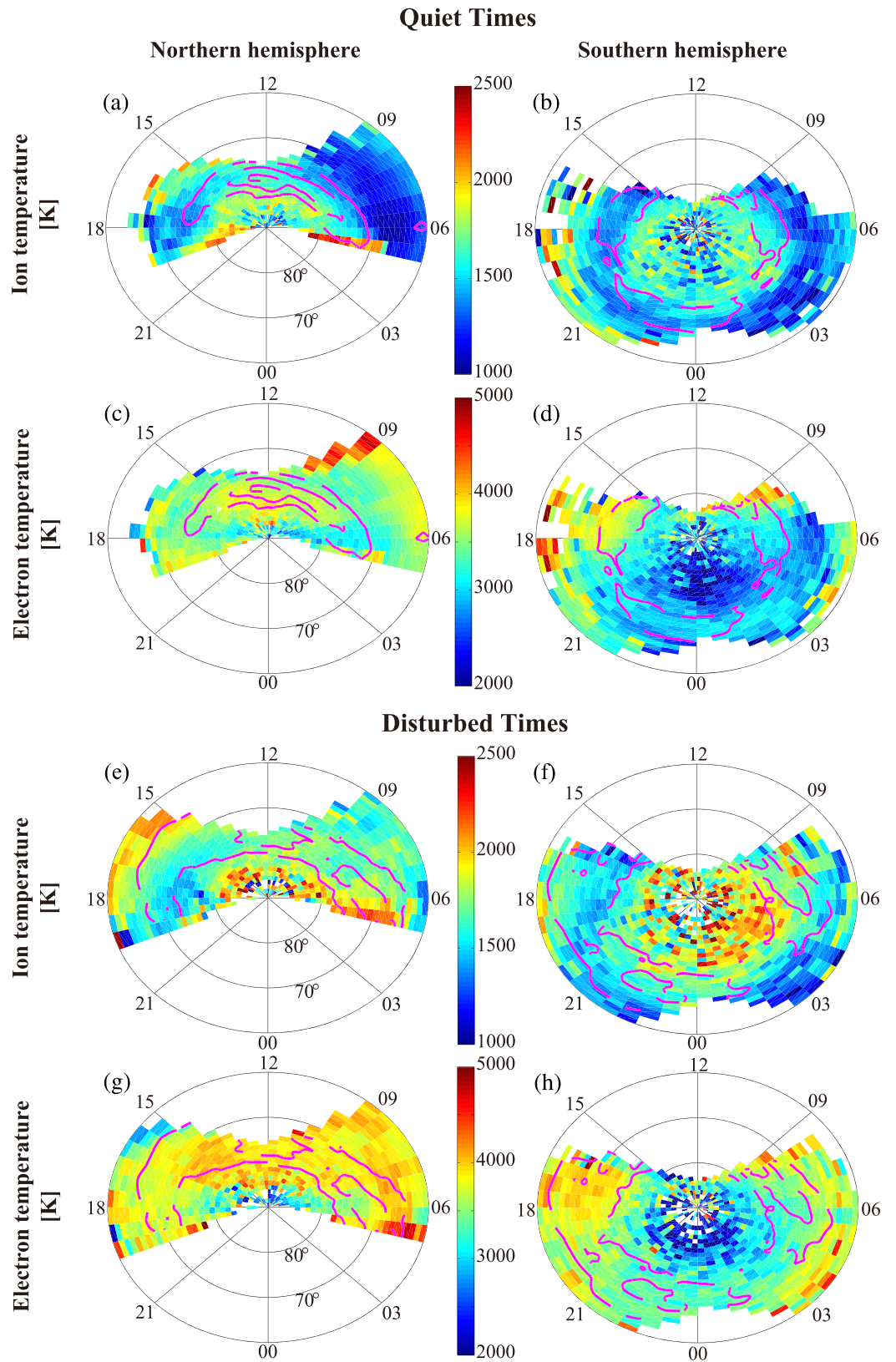


Figure 4. Statistical results of ion and electron temperature in both hemispheres during the selected ion upflow events both for magnetic quiet and disturbed times. The top two rows (a–d) show the data for quiet times and bottom two rows (e–h) show the data for disturbed times.

driven by plasma convection causes ion temperature increase. The increased ion temperature then creates the vertical pressure gradient to produce upward motion of the plasma in the F region ionosphere (e.g., Keating et al., 1990). On the duskside, the upward Region 1 FACs are associated with discrete aurora and soft electron precipitations (electron heating), which could heat up electrons in the F region and topside ionosphere to cause their upward motion. These upwelling heated electrons can pull the ions upward through the ambipolar electric field due to the separation between electrons and ions (e.g., Horwitz & Moore, 1997; Knudsen et al., 1998; Ogawa & Kogawa, 2002; Strangeway et al., 2005).

In order to discuss which heating (ion or electron heating) is more efficient to generate the ion upflow, we also plotted the distributions of the ion and electron temperatures for the selected upflow events in Figure 4 using the same format as Figures 2 and 3. The top two panels in Figure 4 show the data during quiet times, and the bottom two panels show the data during disturbed times. Figure 4 shows that the ion and electron temperature around the area of higher upflow occurrence also has a clear dawn-dusk asymmetry: The electron temperature increased and ion temperature decreased in the dusk sectors (15–18 MLT); in the postmidnight sectors (1–5 MLT), the ion temperature enhanced but electron temperature decreased, while both ion and electron temperature enhanced in the prenoon section (5–9 MLT), noon section, and premidnight section (19–24 MLT). This suggests that ion heating can be important for the generation of ion upflow in the postmidnight sector and electron heating is important in the dusk sector. Both the ion and electron temperatures are elevated in the noon cusp region, prenoon section, and premidnight section, which also overlaps the area of high upflow occurrence. This suggests that the upflow acceleration is more efficient when both ion heating and electron heating contribute in parallel. Figure S1 shows the relationship between ion upflow and electron precipitation, electron temperature, electron/ion temperature difference, and convection speeds. It suggests again that the electron heating associated with precipitating electrons and ion heating from increased convection speed both contribute to ion upflow. The electron/ion temperature difference also influences the upflow velocity, in agreement with the suggestions of Ma, Zhang, Xing, Jayachandran, et al. (2018) and Ma, Zhang, Xing, Heelis, et al. (2018).

The enhanced ion upflow in the cusp region can result from heating and may also in part be due to enhanced flow shears associated with the cusp FAC system. Our results also show an intensification and equatorward expansion of the entire current system and upflow occurrence during disturbed times, which is consistent with EISCAT observations (Fontaine & Peymirat, 1996). We note that the FACs themselves are not driving the ion upflow but indicate that the phenomena are closely related.

Acknowledgments

This work was supported by the National Natural Science Foundation (Grant Nos. 41574138, 41874170, 41604139, 41831072, and 41431072) and the Foundation of National Key Laboratory of Electromagnetic Environment (Grants 6142403180103 and 6142403180102). KO was supported by funding from the Research Council of Norway Grant 223252. We also thank the NOAA FTP and JHU/APL for providing the DMSP data (<https://satdat.ngdc.noaa.gov/dmosp/data/>). The authors also wish to thank the International Space Science Institute in Beijing (ISSI-BJ) for supporting and hosting the meetings of the International Team on “Multiple-instrument observations and simulations of the dynamical processes associated with polar cap patches/aurora and their associated scintillations”, during which the discussions leading/contributing to this publication were initiated/held.

References

- Abe, T., Whalen, B. A., Yau, A. W., Horita, R. E., Watanabe, S., & Sagawa, E. (1993). EXOS D (Akebono) superthermal mass spectrometer observations of the polar wind. *Journal of Geophysical Research*, *98*(A7), 11,191–11,203. <https://doi.org/10.1029/92JA01971>
- Akasofu, S. I., & Kan, J. R. (2013). The boundary of the polar cap and its relation to electric fields, field-aligned currents, and auroral particle precipitation. *American Geophysical Union*, *25*. <https://doi.org/10.1029/GM025p0143>
- Andersson, L., Peterson, W. K., & McBryde, K. M. (2004). Dynamic coordinates for auroral ion outflow. *Journal of Geophysical Research*, *109*, A08201. <https://doi.org/10.1029/2004JA010424>
- Birkeland, K. (1908). The Norwegian Aurora Polaris expedition, 1902–03. Vol. I: On the cause of magnetic storms and the origin of terrestrial magnetism. *Science*, *41*(1044). <https://doi.org/10.1126/science.41.1044.29>
- Chappell, C. R. (1988). The terrestrial plasma source: A new perspective in solar-terrestrial processes from Dynamics Explorer. *Reviews of Geophysics*, *26*(2), 229–248. <https://doi.org/10.1029/RG026i002p00229>
- Chappell, C. R., Giles, B. L., Moore, T. E., Delcourt, D. C., Craven, P. D., & Chandler, M. O. (2000). The adequacy of the ionospheric source in supplying magnetospheric plasma. *Journal of Atmospheric and Solar-Terrestrial Physics*, *62*(6), 421–436. [https://doi.org/10.1016/S1364-6826\(00\)00021-3](https://doi.org/10.1016/S1364-6826(00)00021-3)
- Coley, W. R., & Heelis, R. A. (2009). Stormtime measurements of topside ionospheric upflow from Defense meteorological satellite program. *Journal of Geophysical Research*, *114*, A10305. <https://doi.org/10.1029/2009JA014350>
- Coley, W. R., Heelis, R. A., & Hairston, M. R. (2006). Characteristics of high-latitude vertical plasma flow from the Defense Meteorological Satellite Program. *Journal of Geophysical Research*, *111*, A11314. <https://doi.org/10.1029/2005JA011553>
- Endo, M., Fujii, R., Ogawa, Y., Buchert, S. C., Nozawa, S., Watanabe, S., & Yoshida, N. (2000). Ion upflow and downflow at the topside ionosphere observed by the EISCAT VHF radar. *Annales de Geophysique*, *18*(2), 170–181. <https://doi.org/10.1007/s00585-000-0170-3>
- Fontaine, D., & Peymirat, C. (1996). Large-scale distributions of ionospheric horizontal and field-aligned currents inferred from EISCAT. *Annales de Geophysique*, *14*(12), 1284–1296. <https://doi.org/10.1007/s00585-996-1284-z>
- Fujii, R., Hoffman, R. A., & Sugiura, M. (1990). Spatial relationships between region 2 field-aligned currents and electron and ion precipitation in the evening sector. *Journal of Geophysical Research*, *95*(A11), 18,939–18,947. <https://doi.org/10.1029/JA095iA11p18939>
- Ganguli, G., Keskinen, M. J., Romero, H., Heelis, R., Moore, T., & Pollock, C. (1994). Coupling of microprocesses and macroprocesses due to velocity shear: An application to the low-altitude ionosphere. *Journal of Geophysical Research*, *99*(A5), 8873–8889. <https://doi.org/10.1029/93ja03181>
- Gurnett, D. A., & Frank, L. A. (1973). Observed relationships between electric fields and auroral particle precipitation. *Journal of Geophysical Research*, *78*(1), 145–170. <https://doi.org/10.1029/JA078i001p00145>

- Hardy, D. A., Schmitt, L. K., Gussenhoven, M. S., Marshall, F. J., & Yeh, H. C. (1984). *Precipitating electron and ion detectors (SSJ/4) for the block 5D/Flights 6–10 DMSP (Defense Meteorological Satellite Program) satellites: Calibration and data presentation*. Rep. AFGL-TR-84-0317. Air Force Geophysics Laboratory. <https://satdat.ngdc.noaa.gov/dmsp/docs/AFGL%20-%201984%20-%20F06-F10%20SSJ4%20Cal%20and%20Data%20-%20AFGL-TR-84-0317.pdf>
- Heelis, R. A., Bailey, G. J., Sellek, R., Moffett, R. J., & Jenkins, B. (1993). Field-aligned drifts in subauroral ion drift events. *Journal of Geophysical Research*, *98*(A12), 21,493–21,499. <https://doi.org/10.1029/93JA02209>
- Heelis, R. A., Coley, W. R., Loranc, M., & Hairston, M. R. (1992). Three-dimensional ionospheric plasma circulation. *Journal of Geophysical Research*, *97*(A9), 13,903–13,910. <https://doi.org/10.1029/92JA00872>
- Horwitz, J. L., & Moore, T. E. (1997). Four contemporary issues concerning ionospheric plasma flow to the magnetosphere. *Space Science Reviews*, *80*(1/2), 49–76. <https://doi.org/10.1023/A:1004973603955>
- Iijima, T., & Potemra, T. A. (1976). The amplitude distribution of field-aligned currents at northern high latitudes observed by Triad. *Journal of Geophysical Research*, *81*(13), 2165–2174. <https://doi.org/10.1029/JA081i013p02165>
- Iijima, T., & Potemra, T. A. (1978). Large-scale characteristics of field-aligned currents associated with substorms. *Journal of Geophysical Research*, *83*(A2), 599. <https://doi.org/10.1029/JA083iA02p00599>
- Keating, J. G., Mulligan, F. J., Doyle, D. B., Winsor, K. J., & Lockwood, M. (1990). A statistical study of large field-aligned flows of thermal ions at high-latitudes. *Planetary and Space Science*, *38*(9), 1187–1201. [https://doi.org/10.1016/0032-0633\(90\)90026-M](https://doi.org/10.1016/0032-0633(90)90026-M)
- Khrabrov, A. V., & Sonnerup, B. U. Ö. (1998a). Orientation and motion of current layers: Minimization of the Faraday residue. *Geophysical Research Letters*, *25*(13), 2373–2376. <https://doi.org/10.1029/98gl51784>
- Khrabrov, A. V., & Sonnerup, B. U. Ö. (1998b). Magnetic variance analysis for small-amplitude waves and flux transfer events on a current sheet. *Journal of Geophysical Research*, *103*(A6), 11,907–11,918. <https://doi.org/10.1029/98JA00615>
- Knudsen, D. J., Clemmons, J. H., & Wahlund, J. E. (1998). Correlation between core ion energization, suprathermal electron bursts, and broadband ELF plasma waves. *Journal of Geophysical Research*, *103*(A3), 4171–4186. <https://doi.org/10.1029/97JA00696>
- Li, K., Haaland, S., Eriksson, A., André, M., Engwall, E., Wei, Y., et al. (2012). On the ionospheric source region of cold ion outflow. *Geophysical Research Letters*, *39*, L18102. <https://doi.org/10.1029/2012GL053297>
- Li, K., Haaland, S., Eriksson, A., André, M., Engwall, E., Wei, Y., et al. (2013). Transport of cold ions from the polar ionosphere to the plasma sheet. *Journal of Geophysical Research: Space Physics*, *118*, 5467–5477. <https://doi.org/10.1002/jgra.50518>
- Liang, H. (2006). Ion upflow in the topside polar ionosphere observations by the DMSP satellite. *Chinese Journal of Polar Research*, *18*(2), 98–107. http://en.cnki.com.cn/Article_en/CJFDTOTAL-JDYZ200602003.htm
- Liu, H., & Lu, G. (2004). Velocity shear-related ion upflow in the low-altitude ionosphere. *Annales de Geophysique*, *22*(4), 1149–1153. <https://doi.org/10.5194/angeo-22-1149-2004>
- Liu, H., Ma, S. Y., & Schlegel, K. (2001). Diurnal, seasonal, and geomagnetic variations of large field-aligned ion upflows in the high-latitude ionospheric F region. *Journal of Geophysical Research*, *106*(A11), 24,651–24,661. <https://doi.org/10.1029/2001JA900047>
- Lockwood, M., Chandler, M. O., Horwitz, J. L., Waite, J. H., Moore, T. E., & Chappell, C. R. (1985). The cleft ion fountain. *Journal of Geophysical Research*, *90*(A10), 9736. <https://doi.org/10.1029/JA090ia10p09736>
- Loranc, M., Hanson, W. B., Heelis, R. A., & St. Maurice, J. P. (1991). A morphological study of vertical ionospheric flows in the high-latitude F region. *Journal of Geophysical Research*, *96*(A3), 3627–3646. <https://doi.org/10.1029/90JA02242>
- Luhr, H., Warnecke, J. F., & Rother, M. K. A. (1996). An algorithm for estimating field-aligned currents from single spacecraft magnetic field measurements: A diagnostic tool applied to freja satellite data. *IEEE Transactions on Geoscience and Remote Sensing*, *34*(6), 1369–1376. <https://doi.org/10.1109/36.544560>
- Ma, Y.-Z., Zhang, Q.-H., Xing, Z.-Y., Heelis, R. A., Oksavik, K., & Wang, Y. (2018). The ion/electron temperature characteristics of polar cap classical and hot patches and their influence on ion upflow. *Geophysical Research Letters*, *45*, 8072–8080. <https://doi.org/10.1029/2018GL079099>
- Ma, Y.-Z., Zhang, Q.-H., Xing, Z.-Y., Jayachandran, P. T., Moen, J., Heelis, R. A., & Wang, Y. (2018). Combined contribution of solar illumination, solar activity, and convection to ion upflow above the polar cap. *Journal of Geophysical Research: Space Physics*, *123*, 4317–4328. <https://doi.org/10.1029/2017JA024974>
- Moore, T. E., Lundin, R., Alcayde, D., André, M., Ganguli, S. B., Temerin, M., & Yau, A. (1999). Source processes in the high-latitude ionosphere. *Space Science Reviews*, *88*(1/2), 7–84. <https://doi.org/10.1023/A:1005299616446>
- Nilsson, H., Barghouthi, I. A., Slapak, R., Eriksson, A. I., & André, M. (2013). Hot and cold ion outflow: Observations and implications for numerical models. *Journal of Geophysical Research: Atmospheres*, *118*, 105–117. <https://doi.org/10.1029/2012JA017975>
- Ogawa, Y., Buchert, S. C., Fujii, R., Nozawa, S., & Eyken, A. P. V. (2009). Characteristics of ion upflow and downflow observed with the European Incoherent Scatter Svalbard radar. *Journal of Geophysical Research: Space Physics*, *114*, 1588–1593. <https://doi.org/10.1029/2008JA013817>
- Ogawa, Y., Buchert, S. C., Sakurai, A., Nozawa, S., & Fujii, R. (2010). Solar activity dependence of ion upflow in the polar ionosphere observed with the European Incoherent Scatter (EISCAT) Tromsø UHF radar. *Journal of Geophysical Research*, *115*, A07310. <https://doi.org/10.1029/2009JA014766>
- Ogawa, Y., & Kogawa, Y. (2002). *Generation mechanisms of ion upflow in the polar topside ionosphere* (PhD thesis). Japan: Nagoya University. <http://ir.nul.nagoya-u.ac.jp/jspui/bitstream/2237/6366/1/ko5386.pdf>
- Oieroset, M., Yamauchi, M., Liska, L., & Hultqvist, B. (1999). Energetic ion outflow from the dayside ionosphere: Categorization, classification, and statistical study. *Journal of Geophysical Research*, *104*(A11), 24,915–24,927. <https://doi.org/10.1029/1999JA900248>
- Potemra, T. A. (2013). Relationships between field-aligned currents, electric fields, and particle precipitation as observed by Dynamics Explorer-2. In *Magnetospheric Currents, Geophysical Monograph Series* (pp. 96–103). Washington, DC: American Geophysical Union.
- Qing-He, Z., Zong, Q.-G., Lockwood, M., Heelis, R. A., Hairston, M., Liang, J., et al. (2016). Earth's ion upflow associated with polar cap patches: Global and in situ observations. *Geophysical Research Letters*, *43*, 1845–1853. <https://doi.org/10.1002/2016GL067897>
- Rich, F. J., & Hairston, M. (1994). Large-scale convection patterns observed by DMSP. *Journal of Geophysical Research*, *99*(A3), 3827–3844. <https://doi.org/10.1029/93JA03296>
- Shelley, E. G., Johnson, R. G., & Sharp, R. D. (1972). Satellite observations of energetic heavy ions during a geomagnetic storm. *Journal of Geophysical Research*, *77*(31), 6104–6110. <https://doi.org/10.1029/JA077i031p06104>
- Shelley, E. G., Sharp, R. D., & Johnson, R. G. (1976a). He⁺⁺ and H⁺ flux measurements in the day side cusp: Estimates of convection electric field. *Journal of Geophysical Research*, *81*(13), 2363–2370. <https://doi.org/10.1029/JA081i013p02363>
- Shelley, E. G., Sharp, R. D., & Johnson, R. G. (1976b). Satellite observations of an ionospheric acceleration mechanism. *Geophysical Research Letters*, *3*(11), 654–656. <https://doi.org/10.1029/GL003i011p00654>

- Shen, Y., Knudsen, D. J., Burchill, J. K., Howarth, A., Yau, A., Redmon, R. J., et al. (2016). Strong ambipolar-driven ion upflow within the cleft ion fountain during low geomagnetic activity. *Journal of Geophysical Research: Space Physics*, *121*, 6950–6969. <https://doi.org/10.1002/2016JA022532>
- Shi, J. K., Cheng, Z. W., Zhang, T. L., Dunlop, M., Liu, Z. X., Torkar, K., et al. (2010). South-north asymmetry of field-aligned currents in the magnetotail observed by Cluster. *Journal of Geophysical Research*, *115*, A07228. <https://doi.org/10.1029/2009JA014446>
- Sonnerup, B. U. Ö., & Jr, L. J. C. (1967). Magnetopause structure and attitude from Explorer 12 observations. *Journal of Geophysical Research*, *72*(1), 171–183. <https://doi.org/10.1029/JZ072i001p00171>
- Strangeway, R. J., Ergun, R. E., Su, Y.-J., Carlson, C. W., & Elphic, R. C. (2005). Factors controlling ionospheric outflows as observed at intermediate altitudes. *Journal of Geophysical Research*, *110*, A03221. <https://doi.org/10.1029/2004JA010829>
- Torbert, R. B., Cattell, C. A., Mozer, F. S., & Meng, C. (1981). The boundary of the polar cap and its relation to electric fields, field-aligned currents, and auroral particle precipitation. In S. Akasofu, & J. Kan (Eds.), *Physics of Auroral Arc Formation* (pp. 143–153). Washington, DC: American Geophysical Union.
- Wang, H., Lühr, H., & Ma, S. Y. (2005). Solar zenith angle and merging electric field control of field-aligned currents: A statistical study of the Southern Hemisphere. *Journal of Geophysical Research*, *110*, A03306. <https://doi.org/10.1029/2004JA010530>
- Whitaker, J. H. (1977). The transient response of the topside ionosphere to precipitation. *Planetary and Space Science*, *25*(8), 773–786. [https://doi.org/10.1016/0032-0633\(77\)90129-5](https://doi.org/10.1016/0032-0633(77)90129-5)
- Yeh, H., & Foster, J. C. (1990). Storm time heavy ion outflow at mid-latitude. *Journal of Geophysical Research*, *95*(A6), 7881–7891. <https://doi.org/10.1029/JA095iA06p07881>
- Zhang, Q.-H., Ma, Y. Z., Jayachandran, P. T., Moen, J., Lockwood, M., Zhang, Y. L., et al. (2017). Polar cap hot patches: Enhanced density structures different from the classical patches in the ionosphere. *Geophysical Research Letters*, *44*, 8159–8167. <https://doi.org/10.1002/2017GL073439>
- Zhao, K., Chen, K. W., Jiang, Y., Chen, W. J., Huang, L. F., & Fu, S. (2017). Latitude dependence of low-altitude O⁺ ion upflow: Statistical results from FAST observations. *Journal of Geophysical Research: Space Physics*, *122*, 9705–9722. <https://doi.org/10.1002/2017JA024075>
- Zhao, K., Jiang, Y., Chen, K. W., & Huang, L. F. (2016). Geomagnetic and solar activity dependence of ionospheric upflowing O⁺: FAST observations. *Astrophysics and Space Science*, *361*(9), 295. <https://doi.org/10.1007/s10509-016-2872-3>
- Zhao, K., Jiang, Y., Ding, L. G., & Huang, L. F. (2014). Statistical analysis of outflow ionospheric O⁺ on the declining phase of solar cycle 23 using Fast observations. *Planetary and Space Science*, *101*, 170–180. <https://doi.org/10.1016/j.pss.2014.07.003>
- Zmuda, A. J., Martin, J. H., & Heuring, F. T. (1966). Transverse magnetic disturbances at 1100 kilometers in the auroral region. *Journal of Geophysical Research*, *71*(21), 5033–5045. <https://doi.org/10.1029/JZ071i021p05033>